



Emissions Inventory for Rice Straw Open Burning in Taiwan Based on Burned Area Classification and Mapping Using Formosat-2 Satellite Imagery

Chih-Hua Chang^{1,2,3*}, Cheng-Chien Liu^{3,4}, Ping-Yu Tseng⁴

¹ Department of Environmental Engineering, National Cheng Kung University, Tainan 701, Taiwan

² Sustainable Environment Research Center, National Cheng Kung University, Tainan 701, Taiwan

³ Global Earth Observation and Data Analysis Center, National Cheng Kung University, Tainan 701, Taiwan

⁴ Department of Earth Sciences, National Cheng Kung University, Tainan 701, Taiwan

ABSTRACT

Rice straw open-field burning is practiced in many countries and has been proven to be a significant source of emissions during the harvest season. Current approaches to obtain the fraction of rice straw subject to open burning vary significantly, and can lead to incorrectly estimating air pollutant emissions. This study proposes a remote sensing approach by classifying high-resolution imagery taken by Formosat-2 (FS-2) to map burned areas of rice paddy fields during harvest season to provide visualized and accurate estimations. We requested FS-2 image acquisition over the Chianan Plain, which is the greatest rice-producing area of Taiwan, during 3 weeks following the harvesting of the fall crops in 2009. Simultaneously, a mobile team on the ground examined the state of the rice paddies when FS-2 was scheduled to take the images. Based on these data, a procedure that integrated a ground truth-based classification scheme, land use data, spectral signatures, and supervised decision rules was applied to identify burned sites. The results were verified using the field data, with an overall accuracy of 87% for distinguishing among the 6 cover types of rice paddies, showing that 27.3% of the paddies within the study area were openly burned. Based on the mapping results, a comprehensive inventory of the air pollutant emissions from straw open burning in Taiwan is presented. To facilitate the management of emission sources and to improve local air quality, we encourage the use of FS-2 imaging to monitor the open burning of rice straw.

Keywords: Formosat-2; Straw open burning; Emission inventory; Remote sensing.

INTRODUCTION

The burning of crop residues in fields is one of the most significant activities of global biomass burning (excluding biofuels; Streets *et al.*, 2003), and contributes substantially to air pollution. This is particularly true for the treatment of rice straw in Asian countries, where more than 1.2 million km² of land is used to grow rice, accounting for 60% of rice production worldwide, and there are 2 annual growing seasons. After harvesting, the waste rice straw is frequently burned in the open in regions with insufficient time before planting the next crop to remove and dispose of it in a more controlled manner, such as in a furnace or by using another closed burning technique (Calvo *et al.*, 2011). In addition, some farmers believe that rice straw open burning (RSOB) can remove weeds, control diseases, and release nutrients

for the next crop (Gadde *et al.*, 2009). However, in contrast to closed burning, the open burning of rice straw is an uncontrolled combustion process in which the products of burning are emitted into the atmosphere, such as CO₂, CO, CH₄, PM, NO_x, and SO₂, influencing both the local air quality and global climate (Ito and Penner, 2004; Tipayarom and Oanh, 2007; Viana *et al.*, 2008; Hossain and Park, 2012). Furthermore, burning rice straw in fields may contribute to the emission of harmful air pollutants, such as PAH, PCDDs, and PCDFs, threatening human health (Chen *et al.*, 2008; Shih *et al.*, 2008; Lai *et al.*, 2009; Estrellan and Iino, 2010). In Taiwan, open burning was voted as being 1 of the 3 air pollution activities that should be strictly controlled by residents in 11 of the 25 administrative districts (TWEPA, 2007). Regions with a high density of paddy fields, such as Yunlin County, Chayi County, and Tainan City, were among these 11 areas. Consequently, numerous studies at local and global levels have been performed regarding the monitoring and estimation of air pollutant emissions caused by RSOB (Streets *et al.*, 2003; Ito and Penner, 2004; Gadde *et al.*, 2009; Estrellan and Iino, 2010; Liu *et al.*, 2011). Based on the results of these studies, control strategies and management

* Corresponding author. Tel.: +886-6-275-7575 ext. 65826;
Fax: +886-6-275-2790
E-mail address: chihhua@mail.ncku.edu.tw

policies can be implemented to reduce air pollution.

Determining the quantity of rice straw that is subject to open burning is the basis for estimating the related air pollutant emissions (Gadde *et al.*, 2009), assessing the influence of toxic emissions (Estrellan and Iino, 2010), managing available biofuel resources (Elmore *et al.*, 2008), and approximating the emissions inventory (Kanabkaew and Oanh, 2011). However, current approaches to obtaining the percentage of straw burned in the field are relatively indeterminate, and may lead to uncertain estimations (Venkataraman *et al.*, 2006) and incorrect decisions. First, RSOB typically occurs in vast regions within 1–2 weeks of harvesting. Traditional survey methods (e.g., sending patrolmen to fields or distributing questionnaires to local farmers and residents) provide limited information for spatiotemporal coverage. Second, because of the declining air quality, the estimates from local surveys may be biased because farmers tend to conceal the truth regarding RSOB. For example, although air pollution problems from RSOB remain one of the leading public concerns in Taiwan, agricultural agencies claim that this type of burning only contributes a limited amount of emissions. Therefore, the percentage of straw that is subject to open burning, abbreviated as *B* in the calculation of pollutant emissions (Streets *et al.*, 2003; Kanabkaew and Oanh, 2011), is typically based on educated estimations (Hao and Liu, 1994; Gadde *et al.*, 2009), with the values being extremely uncertain and having a wide range in the reported data (Kanabkaew and Oanh, 2011). Consequently, a monitoring approach that can better “visualize” the *B* value from both temporal and spatial perspectives is significance.

Satellite remote sensing provides a method to create 2D synoptic views and low- or high-frequency observations over long periods, which may be capable of visualizing RSOB-related activities, thereby enabling more accurate estimations. For example, the burned area derived from the VEGETATION instrument onboard Système Pour l'Observation de la Terre (SPOT) 4 satellite (GBA-2000) (Gregoire *et al.*, 2003) has been used to estimate global burned biomass that is associated with open vegetation fires at a 1 km² (1 × 1 km) resolution (Ito and Penner, 2004). The hotspots of active fires detected by the mid-infrared and thermal wavebands of the moderate resolution imaging spectroradiometer (MODIS) onboard the Terra and Aqua satellites provides the opportunity to have a direct matching of daily fire counts at a 1 km² grid resolution (Justice *et al.*, 2002) and has been applied to catalogue emissions from open biomass burning in India (Venkataraman *et al.*, 2006). However, in Asian countries, the size of a rice paddy field commonly ranges from one-half to several hectares, which is considerably smaller than the spatial scale of satellites with 1 km² resolutions, which can cause mixed pixel problems in image classification. In addition, short-lived fires, such as manufactured RSOBs that occur during the gaps between satellite repeat cycles, frequently fail to be included in active fire data (Kanabkaew and Oanh, 2011). Therefore, although remote sensing is of practical use in determining global biomass burning, thus far it has not been applied to the estimation of RSOB on a regional scale.

Image classification based on visible bands provides an alternative method for detecting the burnt areas of RSOB, such as by directly labeling rice paddies with a burned black color in satellite images. The advantage of visible band-based classification is that it can easily be applied to most satellite images. Furthermore, the accuracy and specificity of classification on a regional scale can be enhanced by the use of high spatial resolution images and available GIS data, such as land-use data or the cadasters of rice paddies (Lau and Shiao, 1998). Formosat-2 (FS-2) is the first satellite with a high spatial resolution sensor (2 m in panchromatic, PAN) to be placed in a daily revisit orbit (i.e., 1 day of repeating cycles). It is the second satellite owned and operated by the National Space Organization (NSPO) of Taiwan. Studies have demonstrated the potential of FS-2 for site surveillance (Liu, 2006), rapid disaster response detection (Liu *et al.*, 2009a), illegal gravel mining (Liu *et al.*, 2009b), and environmental monitoring (Chang *et al.*, 2009; Liu *et al.*, 2009c), supporting the use of FS-2 imagery for monitoring RSOB and visualizing the *B* value in Taiwan.

This study demonstrates the combined use of FS-2 imagery and land-use data as the basis for deriving a map of RSOB areas in Taiwan. Consequently, a supervised image classification algorithm was trained and verified by a mobile team during 3 weeks in the harvest of the fall crop season in 2009. These maps enable a better understanding of the temporal and spatial variability of rice straw burning in the studied area. The percentage of rice straw subject to open burning (*B* value) during the fall crop season in 2009 was obtained using the derived RSOB map and by comparing these results to other regionally specific data in Asia. In addition, based on the newly estimated *B* value and reported data, we updated the database of the emission inventory (EI) for RSOB in Taiwan. Air pollutants included in the new EI are CO₂, CO, CH₄, N₂O, NO_x, SO₂, NMHC, EC, OC, PM_{2.5}, PM₁₀, PCDD/Fs, and total PAHs.

MATERIALS AND METHODS

Study Area

The Chianan Plain is an alluvial plain located in the central-southern region of Western Taiwan (Fig. 1). Because of the rich soils and the suitable climate conditions, the Chianan Plain is the highest rice-producing area in Taiwan according to the density of rice paddy fields and greatest rice production, with 2 growing seasons per year. The first growing season in the Chianan Plain typically begins at the end of December, and the harvest is from the end of June to mid-July. The second growing season begins 15–20 days after the first season has ended, and the harvest is from mid-November to early December. As shown in Fig. 1, the Chianan Plain is located in Changhua County, Yunlin County, Chiayi County, and Tainan City, where, during the harvest season, residents frequently complain that RSOB is the most serious source of air pollution (TWEPA, 2007). Furthermore, in addition to direct health effects, the smoke caused by open burning near roads can reduce drivers' perception, causing accidents.

An 8600-ha area in the northern part of Chiayi County

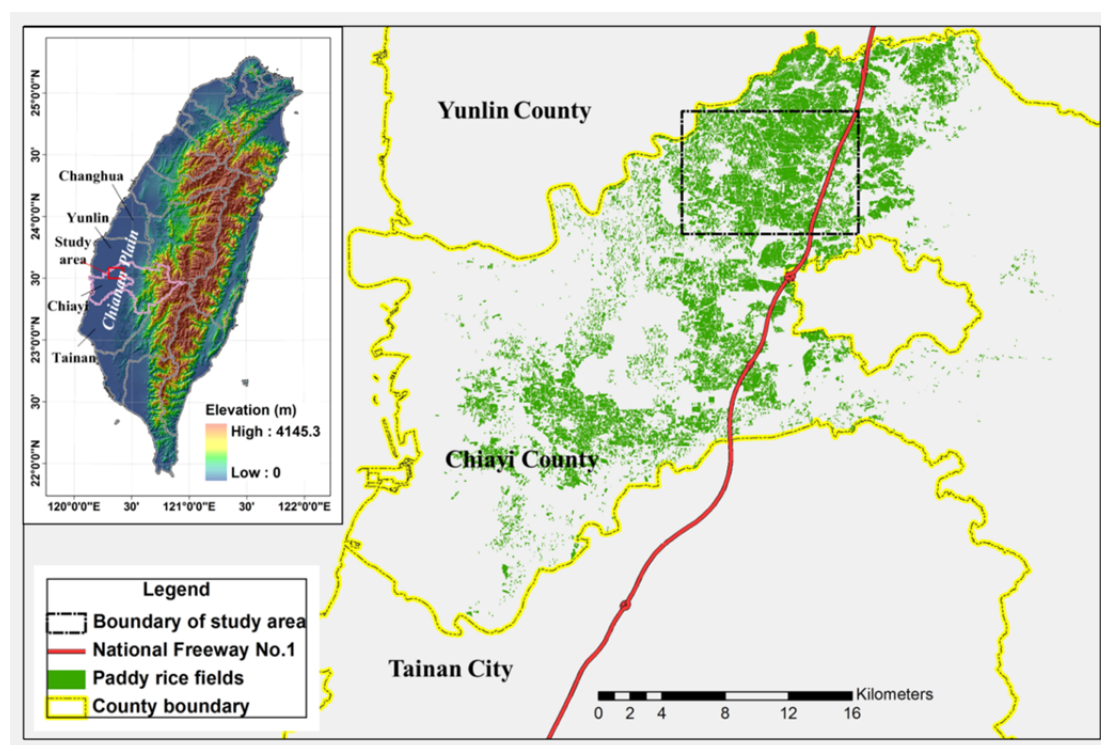


Fig. 1. The location of the test site and map of paddy rice fields in Chiayi County.

was selected as the study area. A total of 4660 ha of rice was planted in the study area during the second growing season of 2009, which was 25% and 4.5% of the total area planted in Chiayi County and Taiwan, respectively. As shown in Fig. 1, the study area is notable for the intensive farming of paddy rice and the presence of the busiest highway in Taiwan (i.e., National Freeway No. 1). In addition, the site was selected because its entire area is just sufficient to be covered on the second of the 7 FS-2 swaths covering Taiwan, negating the need for image merging (Chang *et al.*, 2009), and can be surveyed by a mobile team on the ground within several hours.

Formosat-2 Image Acquisition and Pre-Processing

FS-2 is the second satellite owned and operated by the NSPO of Taiwan. The FS-2 imagery is available for 2 m resolution in panchromatic (PAN) and 8 m resolution in 4 multispectral (MS) bands ranging from visible to near-infrared, with scene coverage of 24×24 km. Table 1 shows the spectral specifications and spatial resolution of the remote sensing imager (RSI) onboard the FS-2. Images taken by FS-2 can be purchased from 4 image distribution centers in Taiwan or from an international company (NSPO, 2012). FS-2 was the first satellite with a high spatial resolution sensor placed in a daily revisit orbit, and therefore, can take daily images of any accessible area in the world. The availability of daily images for a particular area is uncertain and depends on the weather conditions and job priority of the NSPO. For example, although we requested intensive FS-2 image acquisition during the study period (11/15/2009–12/6/2009), only 2 clear images were successfully taken at the end of the harvest season (12/3/2009 and 12/4/2009).

Image acquisition was unavailable for days with cloud cover and from 11/20/2009 to 11/27/2009, when FS-2 underwent a 1 week emergency maintenance.

All raw images were preprocessed by the automatic Formosat-2 image processing system (F2-AIPS; Liu, 2006), including band-to-band coregistration (Liu *et al.*, 2007), orthorectification (Liu and Chen, 2009), geometrical registration of the multi-temporal imagery (Liu *et al.*, 2009b), and radiometric normalization of the multi-temporal imagery (Chang *et al.*, 2009). Following image orthorectification, a root mean square error (RMSE) of 1.5 pixels (3 m) for the geometrical registration was obtained using F2-AIPS.

Integrating GIS Data and Ground Survey for Image Classification

The basis of multispectral image classification is the automatic categorization of all pixels in an image into several land cover classes based on the spectral patterns (Lillesand *et al.*, 2004). Depending on the complexity of the land covers, a set of spectra classes may be composed of various types of land uses (e.g., urban and agriculture), stages of a certain use (e.g., paddies and harvested paddies), or special activities on the ground (e.g., burned and unburned crops). To obtain significant information relevant to RSOB and to enhance the overall classification accuracy, strategies to narrow the range of possible classes to be classified and to identify cover types of interest were used, respectively.

Land Use Data Integration

Land use information is the description of how people use land, which is distinct from the term land cover. The information is commonly collected using remote sensing

Table 1. The specifications of Formosat-2 and the RSI instrument.

Formosat-2 Orbit Information	Launch date	2004/05/21	
	Orbital Altitude	891 km	
	Orbital Inclination	98.99°, sun-synchronous	
	Speed	6.5 km/sec	
	Orbit Time	102.86 minutes	
	Revisit interval	Daily	
	Crossing time	AM 9:40, PM 9:40 (Taiwan local time)	
Formosat-2 RSI Specifications	Image bands	Panchromatic (PAN)	0.45–0.82 μm
			0.45–0.52 μm (Blue)
		Multi-spectral (MS)	0.52–0.60 μm (Green)
			0.63–0.69 μm (Red)
			0.76–0.90 μm (NIR)
	Resolution (nadir)	PAN: 2 m, MS: 8 m	
	Swath (nadir)	24 km	
	Imaging system	Pushbroom scanner	
	Viewing angles	Cross-track and along-track (forward/aft): $\pm 45^\circ$	

tools and field surveys (Comber *et al.*, 2005). For enhanced resource management and planning, land use surveys in Taiwan are routinely performed by the National Land Surveying and Mapping Center (NLSC) of the Ministry of the Interior. The most recent national land use survey was performed from 2006 to 2008 using aerial imaging technology, auxiliary GIS data, and ground surveying (NLSC, 2011). The land use map of our study area, Chiayi County, was produced in 2007, and has a map scale of 1:5000. We assumed that the differences between the land use in 2007 and when this study was conducted (2009) were negligible. The feature class of rice paddy in the land use map was considered a boundary confining the is-rice pixels in the image, and the not-rice pixels were masked out of the image.

Training Areas and Classification Scheme

Following the masking procedure, the range of targets to be classified was narrowed to a single use: rice paddy. As mentioned, there were various cover types for rice paddies within the transition time between the harvest and regrowing. A classification scheme that can cover types relevant to “burned area” is imperative to estimate the fraction of rice straw subject to open burning. For example, if only the 2 categories of “crop” and “burned crop” are available in the classification scheme, fields in which the soil is being prepared for the next season may be mistaken for “burned areas” because their surface spectral feature (color) is closer to a “burned crop” than to a “crop.” In this case, the caused error of inclusion would overestimate the *B* value. In addition, the *B* value is underestimated because of the error of exclusion if a parcel of burned field with weed regrowth is mistaken for “crop.” Consequently, this study proposes a ground truth-based classification scheme to reduce these errors and increase the overall accuracy.






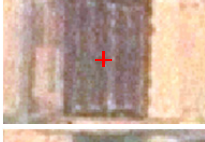






While FS-2 was taking images of the study area, 43 representative training areas were identified by the ground team to compile a numerical signature file for the supervised classification. The training areas were identified by taking photographs and locating the center point of the paddy with a handheld GPS. By visually comparing the field data

and corresponding FS-2 image collected in training areas, a classification scheme with 6 cover types was constructed, as listed in Table 2. Pixels that were insufficiently similar to any of the listed types following the supervised classification were labeled “unknown.” The proposed scheme was merely used to spectrally distinguish each pixel from among classes that could not cause additional errors in classifying the primary burned areas (i.e., Types C and D). The scheme was not intended to statistically cover all of the possible themes that can occur within a harvest and regrowth season. The validity of the scheme can later be confirmed by a classification error matrix resulting from the verification data set.

Supervised Classification with the Maximum Likelihood Function

In the classification stage, the Gaussian maximum likelihood method was used as a decision rule to classify the unknown pixels into appropriate categories. The probability of a given pixel value being a member of a particular theme (i.e., the likelihood function) was rapidly calculated based on the established category spectral response patterns and the normality assumption of the pixels that formed the category training data (Lillesand *et al.*, 2004). The pixel was assigned to the most likely type with the maximum likelihood function or was labeled as unknown if the probability values were all below a set threshold. A high threshold value (meaning that more pixels are classified as unknown) can ensure the accuracy of classification but results in the loss of more information that could be extracted from the image. For example, if the classification target is not diverse and the classification scheme is sufficient to cover most of the pixels, then setting a high threshold value reduces the overall accuracy by increasing the errors of omission. Therefore, rule images that contain classification measures such as the number of matches and probabilities were created during the supervised classification procedure. By referring to these rule images, the lowest threshold value that satisfied the overall classification accuracy was used in this study.

Table 2. The description and ground-truth data for six cover types relevant to RSOB.

Type	Description	Representative ground photo	Typical scene retrieving from the FS-2 image
A	Harvested, but no further actions, neither disposal of straw nor growth of weeds		
B	Growth of weeds in unburned area.		
C	Burned recently, and yet have weeds grown.		
D	Growth of weeds in burned area.		
E	Harvested, disposed and soil prepared for the next growing season.		
F	Not yet harvested.		

Finally, in the verification stage, classification performance was evaluated by comparing the results to other ground-truth data identified in the corresponding verification area by the same mobile team during the study period. Because the team aimed to identify training samples, the fieldwork of positioning and type labeling for the ground-truth data was not performed during the 2 days when FS-2 took the clear images. Both error matrices resulting from the classifying verification set and 3 indicators of accuracy for image classification (i.e., producer accuracy, user accuracy, and overall accuracy) were calculated to quantify the classification performance (Lillesand *et al.*, 2004).

Estimation of the Air Pollutant Emissions from RSOB

Following the generic methodology that the Intergovernmental Panel on Climate Change (IPCC) uses for national greenhouse gas inventories (IPCC, 2006), the emissions of the specific air pollutant i from agricultural and forestry sources for any type of fire can be calculated as

$$E_i = C_f \times G_{ef,i} \times M_B \times 10^{-3} \quad (1)$$

where E_i is the emission of air pollutant i from RSOB in tons/y, C_f is the combustion factor (dimensionless), $G_{ef,i}$ is the emission factor (EF) of pollutant i in g/kg dry matter burnt (g/kg_{dm}), and M_B is the mass of rice straw available for

open burning in tons/y. The C_f value is the measure of the proportion of fuel that is actually combusted, which depends on the size, architecture, crop-specific burn efficiency, and moisture content of the fuel load (IPCC, 2006). The IPCC-recommended C_f value of 0.8 for rice residues was used in this study. Although the IPCC guideline provides recommended values of G_{ef} for general GHGs, these were not specified for rice straw. Therefore, the G_{ef} data used in this study were selected based on a comprehensive review of journal articles and reports. Table 3 lists the selected EFs for GHGs and the conventional and harmful air pollutants associated with straw open burning. EFs that are within the recommended range of the IPCC and constitute the latest data available for rice straw open burning are preferred. Finally, M_B was estimated from the annual production of paddy (i.e., unhusked rice) as

$$M_B = B \times P \times R_{SP}, \quad (2)$$

where B is the fraction of straw subject to open burning (%), P is the annual paddy production (tons/y), and R_{SP} is the rice straw to paddy ratio (dimensionless). As mentioned, the most uncertain part in the estimation of RSOB emissions constitutes the choice of a B value. In this study, the value of B was obtained by the image classification result. The paddy production data are available from the national

Table 3. Summary of EFs reported in the literature and used in this study.

Pollutants	G_{ef} (g/kg _{dm})	Source	Description	EF used in this study
CO ₂	1515 ± 177	(IPCC, 2006)	For agriculture residues	1460
	1460	(Jenkins and Bhatnagar, 1991)	Specific for rice straw open burning, used in Gadde <i>et al.</i> (2009)	
	1177	(Oanh <i>et al.</i> , 2011)	EF determined from field burning of rice straw in Thailand, used in Kanabkaew and Nguyen (2011)	
CO	92 ± 84	(IPCC, 2006)	For agriculture residues	93
	34.7	(Kadam <i>et al.</i> , 2000)	Specific for rice straw, used in Gadde <i>et al.</i> (2009)	
	93	(Oanh <i>et al.</i> , 2011)	EF determined from field burning of rice straw in Thailand, used in Kanabkaew and Nguyen (2011). It is also the latest EF data specific for rice straw.	
CH ₄	2.7	(IPCC, 2006)	For agriculture residues.	1.2
	1.2	(USEPA, 1992)	From the USEPA AP-42 database specific for rice straw, used in Gadde <i>et al.</i> (2009).	
	9.59	(Christian <i>et al.</i> , 2003)	From a laboratory measurement of EF for rice straw burning, used in Kanabkaew and Nguyen (2011).	
N ₂ O	0.07	(IPCC, 2006)	For agriculture residues, used in Gadde <i>et al.</i> (2009).	0.07
NO _x	2.5 ± 10	(IPCC, 2006)	For agriculture residues.	2.28
	2.28	(Cao <i>et al.</i> , 2008)	EF determined from crop residue burning in China, used in Kanabkaew and Nguyen (2011)	
SO ₂	0.18	(Cao <i>et al.</i> , 2008)	EF determined from crop residue burning in China, used in Kanabkaew and Nguyen (2011)	0.18
NMHC	4	(USEPA, 1992)	From the USEPA AP-42 database specific for rice straw, used in Gadde <i>et al.</i> (2009).	4
EC	0.51	(Oanh <i>et al.</i> , 2011)	The latest EF data available for rice straw burning, used in Kanabkaew and Nguyen (2011).	0.51
OC	2.99			2.99
PM _{2.5}	12.95	(Hays <i>et al.</i> , 2005)	Specific for rice straw open burning, used in Gadde <i>et al.</i> (2009)	8.3
	8.3	(Oanh <i>et al.</i> , 2011)	The latest EF data available for rice straw burning, used in Kanabkaew and Nguyen (2011).	
PM ₁₀	3.7	(Kadam <i>et al.</i> , 2000)	Specific for rice straw open burning, used in Gadde <i>et al.</i> (2009)	9.1
	9.1	(Oanh <i>et al.</i> , 2011)	The latest EF data available for rice straw burning, used in Kanabkaew and Nguyen (2011).	
PCDD/Fs	4.86 × 10 ⁻⁸ *	(Lin <i>et al.</i> , 2007)	EF for 17 kinds of PCDD/Fs from open burning of rice straw in Taiwan	4.86 × 10 ⁻⁸ *
	5 × 10 ⁻¹⁰ *	(Gullett and Touati, 2003)	EF determined specific for rice straw open burning in US, used in Gadde <i>et al.</i> (2009).	
ΣPAHs	5.26 × 10 ⁻³	(Zhang <i>et al.</i> , 2011)	A combination of particulate and gaseous emissions factors for 16 kinds of PAHs from rice straw burning	5.26 × 10 ⁻³
	1.86 × 10 ⁻²	(Keshtkar and Ashbaugh, 2007)	Particulate EF determined specific for rice straw open burning in US, used in Gadde <i>et al.</i> (2009).	
*g I-TEQ/kg (International Toxic Equivalents, TEQ)				

statistics agency. According to the annual food statistics report for 2007 to 2010 (Agriculture and Food Agency, 2010), the annual planted area of rice and production paddies averaged 252,944 ha and 1,462,453 tons/y in Taiwan, respectively, during this period. The R_{SP} value ranged from 1.0 to 4.3 depending on the rice variety (Elauria *et al.*, 1999). For the most frequently planted varieties, the value of 1.11, as suggested by the Food and Agriculture Organization of the United Nations (FAO), was used.

RESULTS AND DISCUSSION

Processed Formosat-2 Images

The FS-2 images of the study area taken before 11/10/2009 and after 12/4/2009 for the spring harvest season are shown in Figs. 2(a) and 2(b), respectively. The multispectral images were pan-sharpened to a 2-m spatial resolution and orthorectified to a RMSE of 3 m for geometrical registration. As shown in Fig. 3, the good agreement between the boundary of the rice paddies from the land use data and that shown in the images indicates the high spatial resolution and geometrical accuracy of the processed FS-2 images. This is essential for integrating the vectored GIS data and images to enhance the performance of image classification.

In addition to geometrical accuracy and high resolution, the resulting images provide good visual indication of the burnt area and state of rice paddies in a suitable spectral setting. The change in color of the rice paddies across the harvest period is evident in the multi-date FS-2 images. The dominant yellow-green in the image taken on 11/10/2009 indicates the ripening stage of growth (Fig. 2(a)), which dramatically turns to brown in the image taken 3 weeks later, when most of the paddies had been harvested (Fig. 2(b)). Some of the rice paddies located in the southwestern part of the study area were harvested earlier in the season, indicating a variation in harvest time, and their effects on the classification of the RSOB themes are not discussed in this paper because the number of multi-date images is insufficient. Further research to integrate multi-date imagery change detection and classification would elucidate this issue. As shown in Fig. 2(b), potential RSOB areas can be visually distinguished from images taken after the harvest season by their burned black color.

Training and Verification for Image Classification

During the 2 days when clear FS-2 images were taken, the ground team successfully identified 43 parcels of paddy as training sites, which are shown in the circles in Fig. 2(b). For some particular paddies that contained more than one cover type in a parcel, such as those that were partly burned or contained weeds, the determination was based on what type occupied the largest coverage area. Similarly, in the corresponding image, the pixels within a parcel of paddy could be categorized into various types. Regardless of whether the mixed type of a parcel was attributed to the ground situation or image noise, the type determination for the resulting classification was also based on the coverage area. With a visual examination of paddies that were identified in the concurrent FS-2 image, 831, 864, 933, 932,

1008, and 134 pure pixels were collected as the training samples for Types A, B, C, D, E, and F, respectively. The spectral values (i.e., digital number, DN) for the collected pixels of the same type were averaged and are shown in Fig. 4. Based on the response of the green band, the 6 spectra can be directly classified into 3 groups: Group I (Types A and B), Group II (Types E and F), and Group III (Types C and D). The 2 types relevant to the burned area (i.e., Group III) can be distinguished from the 2 unburned ones (i.e., Group I). In Group II, Type F can be differentiated from Type E by its high green to red ratio. Type E has a similar spectral shape to Type C but has a distinct response in blue. In addition, types with weed growth have a higher green to red ratio, which can be used to differentiate types in the same group, such as Types A and B and Types C and D. The setting of FS-2 visible bands is generally appropriate for the predefined classification scheme.

Using the training data pixels as the numerical signature, the FS-2 image taken on 12/4/2009 was automatically classified using supervised classification with the maximum likelihood decision rule. Because the ground-truth data type was identified on a per parcel basis, the accuracy of classification was evaluated by comparing the classification result to the total 119 parcels of paddy (ground-truth data) within the verification area (Fig. 5). As mentioned, the day the mobile team labeled the verification parcels was not the same as when FS-2 was taking the images for classification. Therefore, the ground-truth data were rechecked again on 12/5/2009 to ensure that the identified labels had not changed. As shown in Fig. 5(a), the verification area contained 57 parcels of paddy labeled Type A, 22 for Type B, 14 for Type C, 19 for Type D, 5 for Type E, and 2 for unknown. No rice paddy was Type F.

By overlapping the labels with the classified map (Fig. 5(b)), the error matrix was constructed based on parcel-by-parcel comparisons between the ground-truth data and the corresponding results of the automated classification. Table 4 lists the error matrix, producer's accuracy, user's accuracy, and the overall accuracy of the classification results. As shown in the error matrix, most of the errors (i.e., non-diagonal elements) were attributable to mistaking Types A for B, Types B for A, and Types C for D. For example, the error matrix indicated that 4 of the 19 parcels that should have been classified as Type D were omitted from that category, resulting in the low producer's accuracy of 79%. In addition, 9 of the 27 parcels that should not have been classified as Type B were included, resulting in the lowest user's accuracy of 67%. An overall accuracy of 87% was achieved and all of individual accuracies were greater than 80%, with the exception of the 2 mentioned cases. A low threshold of 0.01 was attained in the supervised classification, indicating that approximately all of the parcels in the verification area were spectrally distinguishable using the numerical signature and classification scheme. The elements underlined in the error matrix (Table 4) showed that only 1 of the 33 parcels of burned area (Types C and D) was mistaken for the other types, causing a low error rate of 3% and further demonstrating the validity of the purposed classification scheme. The overall accuracy for the *B* value

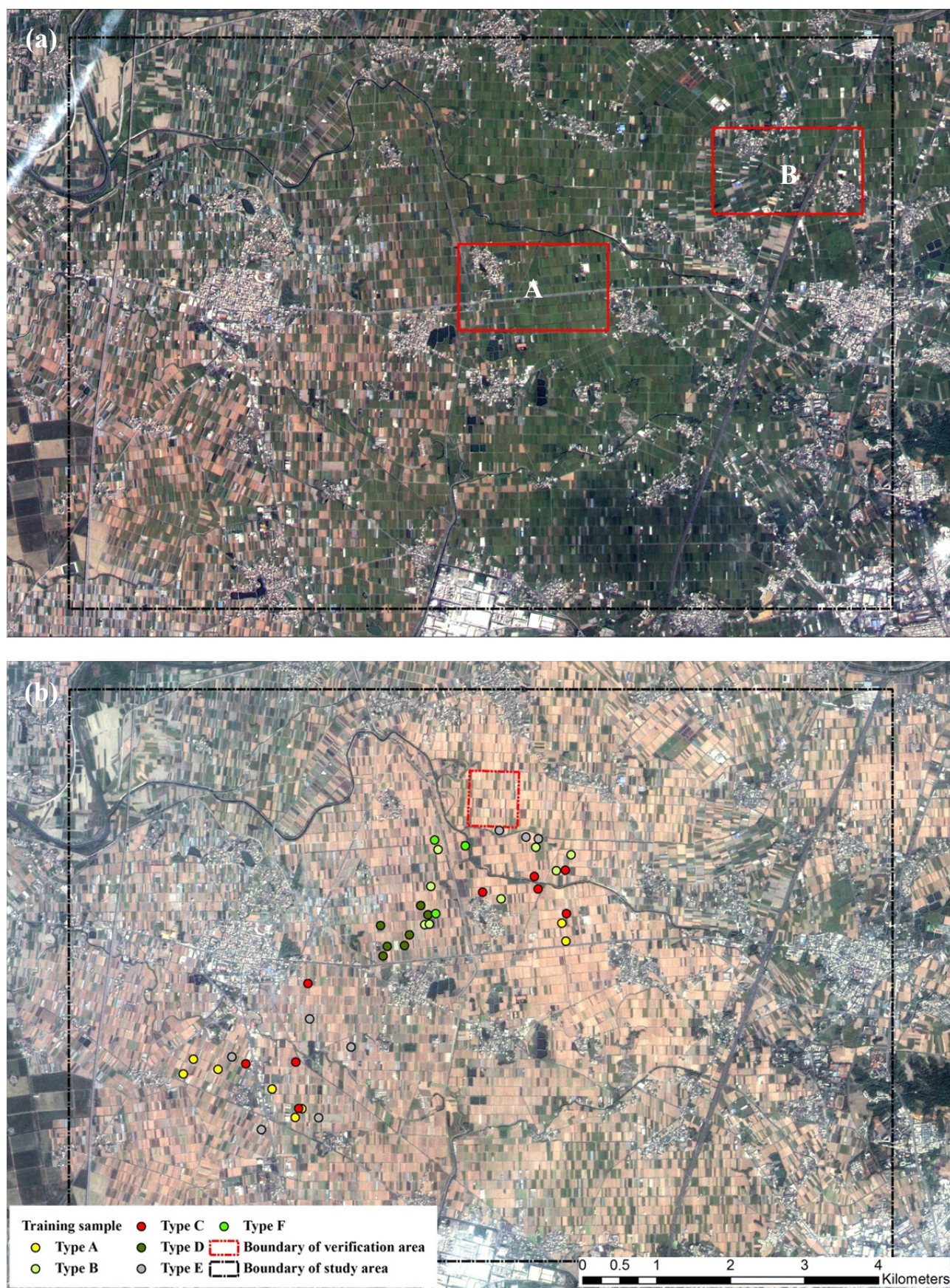


Fig. 2. The true color Formosat-2 images of the study area taken (a) before (11/10/2009), and (b) after (12/4/2009) during the harvest period of the second crop season.



Fig. 3. A near view of the example areas A and B denoted in Fig. 2(a).

estimation increased from 87% to 98% if we ignored the errors (italics and bold elements in the error matrix) that were irrelevant to the classification of burned area.

Estimating the B Value Based on Burned Area Classification and Mapping

Fig. 6 shows the verified results of the image classification for the burnt area mapping during the second harvest season of 2009. In addition, 89% of the total study area was successfully classified into the 6 predefined categories, with Type A at 13.5%, Type B at 27.6%, Type C at 14.0%, Type D at 13.2%, Type E at 19.4%, and Type F at 0.9%. The B value that was estimated from the results of image classification was 27.2% (i.e., a combination of Types C and D).

The comparison of the B values developed in this study and cited in previous literature is listed in Table 5. The B value of 0.27 that was developed in this study is the first visualized result for the percentage of rice straw subject to open burning at the regional level. As one of the most uncertain parameters in the EI (Venkataraman *et al.*, 2006; Kanabkaew and Oanh, 2011), the B value varies considerably regarding where it is derived and the various survey methods. The B value is essentially a country-specific parameter that must be obtained locally (IPCC, 2006). However, the approaches for obtaining B are typically general and inconsistent, which may cause varied estimations. For example, Gadde *et al.* (2009) concluded that the chief reason for the differences in air pollutant emissions from RSOB in their study and that of other studies (Streets *et al.*, 2003)

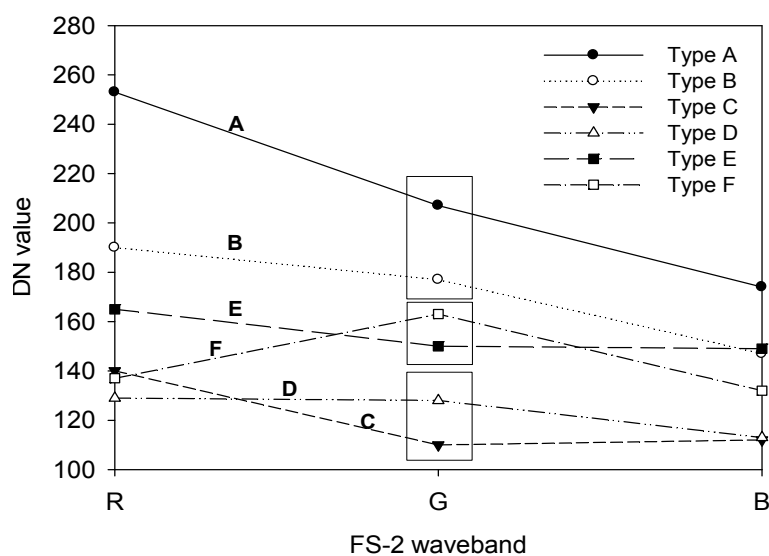


Fig. 4. The spectral attributes for the six cover types in the classification scheme.

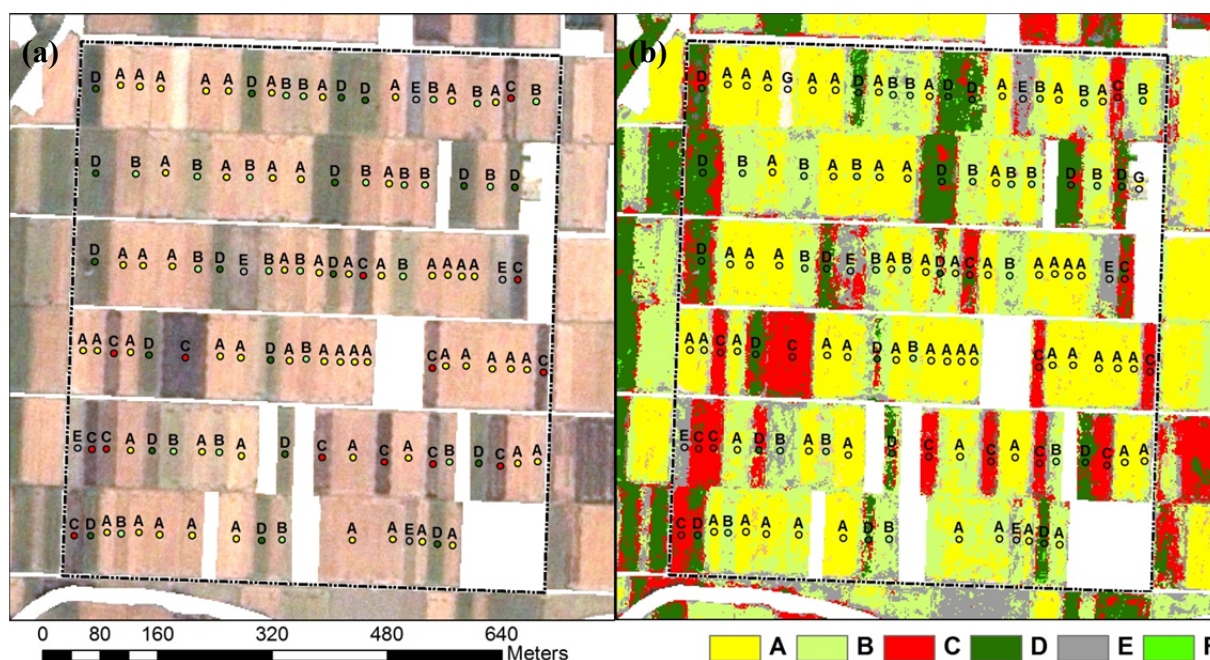


Fig. 5. Verification of the image classification results, (a) the field labeling results of the 119 paddies for land owners within the verification area, and (b) overlapping field labeling with the classification results.

was the methodology they used to estimate the B value, as shown in Table 5. Most of the country-specific data obtained by field surveys [Thailand: Tipayarom and Oanh (2007); The Philippines: Gadde *et al.* (2009)], such as personal interviews and questionnaires, are higher than those reported in government documents [Thailand: Gadde *et al.* (2009); Kanabkaew and Oanh (2011)] or surveyed by a national program [India: Gadde *et al.* (2009)]. Furthermore, B values suggested by the IPCC and estimated at the continental or global level (Hao and Liu, 1994; Streets *et al.*, 2003) were lower than those surveyed at a local or regional scale. In Taiwan, the fraction of RSOB claimed by government agencies occasionally only represents the part of the in-

process burning that has been identified, which may be the reason air pollution problems from RSOB remain a leading public concern (TWEPA, 2007), despite the espoused percentage of RSOB decreasing. For an EI, the B value of 0.27 developed in this study may be more accurate.

Emissions Inventory for Rice Straw Open Burning in Taiwan

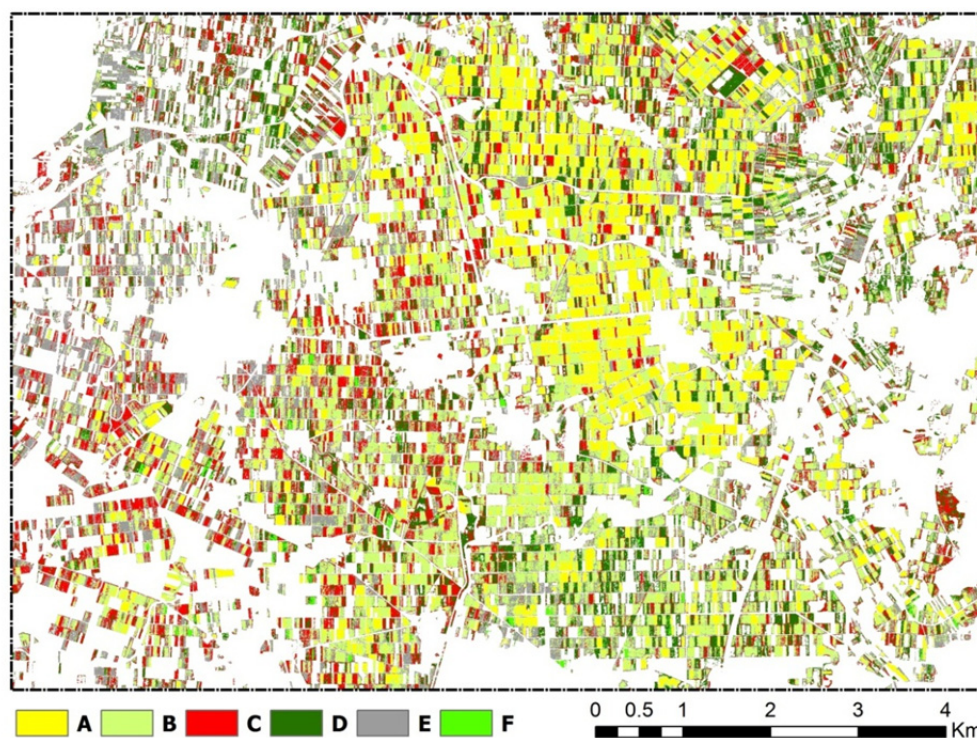
An annual amount of 438,297 tons of rice straw subject to open burning was estimated using Eq. (2) and the B value developed in this study. This is equivalent to 1.73 tons of annual estimate of air pollutant emissions from RSOB was calculated using Eq. (1) and is provided in Table 6. CO_2 is

Table 4. The results of image classification for the verification data.

Classification result	Verification data							Row total	Producer's accuracy	User's accuracy
	A	B	C	D	E	F	Un-known			
A	50	4	0	0	0	0	0	54	88%	93%
B	7	18	0	<u>1</u>	<i>1</i>	0	0	27	82%	67%
C	0	0	14	<u>3</u>	0	0	0	17	100%	82%
D	0	0	0	15	0	0	0	15	79%	100%
E	0	0	0	0	4	0	0	4	80%	100%
F	0	0	0	0	0	0	0	-	-	-
Unknown	0	0	0	0	0	0	2	2	100%	100%
Column total	57	22	14	19	5	-	2	119	Overall acc. = 87%	

Underlined elements: errors relevant to the “burned area” classification.

Italic and bold elements: errors not relevant to the “burned area” classification.

**Fig. 6.** The verified results of FS-2 image classification for the RSOB area mapping that occurred during the second harvest season of 2009.**Table 5.** Summary of the *B* values developed in this study and cited in the literature.

Study area	<i>B</i>	Description and survey methods	Source
Taiwan	0.27	Burned area mapping by FS-2 imagery	This study
	0.10	Obtained by field survey	(Lin <i>et al.</i> , 2007)
India	0.14	Parameter specific for India, by personal communication	(Gadde <i>et al.</i> , 2009)
	0.18–0.30	Derived from the MODIS active-fire data	(Venkataraman <i>et al.</i> , 2006)
Thailand	0.48	Data surveyed by Dept. Alternative Energy Development, Thailand	(Gadde <i>et al.</i> , 2009)
	0.90	Data surveyed in Central Thailand	(Tipayarom and Oanh, 2007)
	0.30	Data surveyed by Energy for Environment Foundation, Thailand	(Kanabkaew and Oanh, 2011)
	0.95	Surveyed by personal interviews and questionnaires	(Gadde <i>et al.</i> , 2009)
Asian countries	0.25	Data for South Asia, by personal communication	(Streets <i>et al.</i> , 2003)
	0.17	Data for rest of Asia, by educated guess	(Hao and Liu, 1994)
Global estimate	0.25	Parameter for developing countries, by expert assessment	(IPCC, 2006)
	< 0.10	Parameter for developed countries, by expert assessment	

Table 6. Air pollutant emissions from straw open burning in Taiwan.

Air pollutants	G_{ef} (g/kg _{dm})	Emissions (tons/yr)
CO ₂	1,460	511,931
CO	93	32,609
CH ₄	1.2	421
N ₂ O	0.07	25
NO _x	2.28	799
SO ₂	0.18	63
NMHC	4	1,403
EC	0.51	179
OC	2.99	1,048
PM _{2.5}	8.3	2,910
PM ₁₀	9.1	3,191
ΣPAHs	5.26×10^{-3}	2
PCDD/Fs	4.86×10^{-8}	1.70×10^{-5} *

*: tons I-TEQ/yr

straw being open-burned annually per hectare of rice paddy. Based on the amount available for open burning, the major gas resulting from RSOB that contributes to the greenhouse effect and is equivalent to emissions from 42,661 people in Taiwan. Chiu *et al.* (2011) indicated that RSOB is a significant PAH emission source because it substantially increases the particulate matter (PM), polycyclic aromatic hydrocarbon (PAH) concentration, and PAH dry deposition in the ambient air of a rice paddy during an open burning event. In this study, the annual emissions from RSOB were estimated to be 6,101 tons of PM (PM₁₀ + PM_{2.5}) and 2 tons of total PAH. In addition, the overall dioxin EI in Taiwan shows that emissions from RSOB are 7.7 g I-TEQ/yr, ranking fourth (8.1%) among the 18 sources we studied (Lin *et al.*, 2007). Based on the new value of *B* developed in this study, the PCDD/Fs emissions from RSOB are estimated to be 17.0 g I-TEQ/y and 16.2% of the total, making it the fourth largest source in Taiwan. However, the percentage of emissions from RSOB is the third highest, exceeding that of iron and steel production, if the *B* value is increased from 0.27 to 0.35. For other pollutants, such as CO, NO_x, SO₂, and NMHC, the contributions from RSOB do not play a significant role in the national emissions (Tipayarom and Oanh, 2007). However, emissions from RSOB have a considerable effect on the local ambient air quality because their occurrence is concentrated in 2 months of the year and confined to specific regions (Yu, 2012).

CONCLUSIONS

RSOB has been proven to be a significant source of air pollution in Taiwan (Shih *et al.*, 2008; Wu *et al.*, 2010; Yu, 2012). However, the answer to how much rice straw is burned in fields is unclear and has perhaps been incorrectly estimated by previous methods. This study developed a remote sensing approach by classifying the FS-2 imagery taken during the rice harvest season to map the burned areas and provide visualized estimation with high accuracy. This novel approach provides a practical and feasible solution to the management of RSOB during the harvest season.

However, the *B* value developed in this study was based on 2 FS-2 scenes over 25% of the area of rice planted in Chiayi County. A study that covers a larger area is required to ensure that the *B* value is representative across Taiwan. The principal conclusions of this study are as follows:

- (1) The RSOB area, including both the paddies recently burned and those with weeds following burning, can be distinguished spectrally from other types by their lower responses in the 3 visible bands of the RSI sensor, particularly in the green band.
- (2) The results of the supervised classification were verified using field data, and an overall accuracy of 98% for identifying the burned areas of rice paddies was achieved, with 27.3% (*B* value) of the paddies in our study area being open-burned during the second harvest season in 2009. The burned area was spatially inconsistent within the study area because of the varied timing of the harvesting. Regions that were harvested early had a higher density of burned sites, less weeds regrowth, and more paddies that had been prepared for the next crop season.
- (3) The *B* value developed here is higher than that suggested by the IPCC and assessed by experts at the global level, but is more comparable to that obtained in other rice-producing countries and mirrors the level of public concern in Taiwan.
- (4) Based on the estimated *B* value, a comprehensive inventory of air pollutant emissions from RSOB in Taiwan was presented in this work, including greenhouse gases, particulate matters, and harmful air pollutants. The results indicate that CO₂ is the primary gas resulting from RSOB that contributes to the greenhouse effect, which is equivalent to the emissions of 42,661 people in Taiwan.
- (5) The *B* value is one of the main parameters that contribute to the uncertainty of the emissions inventory, which can lead to differing management practices. For example, depending on the *B* level, emissions from RSOB may be the third or fourth highest source of PCDD/Fs in Taiwan.

ACKNOWLEDGMENTS

The authors thank the Environmental Protection Bureau of Chiayi County for their financial support for this project and for their assistance with the field investigations. In addition, this study was supported by the National Science Council of the Republic of China, Taiwan, through grants NSC-99-2625-M-006-003, and NSC-100-2625-M-006-005.

REFERENCES

- Agriculture and Food Agency (2010). Taiwan Food Statistic Report, In: Agriculture and Food Agency, Council of Agriculture Executive Yuan, Taiwan, Available from: http://www.afa.gov.tw/content_en.asp?pcatid=1&ycatid=1&lcatid=394.
- Calvo, A.I., Castro, A., Pont, V., Cueto M.J., Sánchez

- M.E. and Fraile, R. (2011). Aerosol Size Distribution and Gaseous Products from the Oven-controlled Combustion of Straw Materials. *Aerosol Air Qual. Res.* 11: 616–629.
- Cao, G.L., Zhang, X.Y., Gong, S.L. and Zheng, F.C. (2008). Investigation on Emission Factors of Particulate Matter and Gaseous Pollutants from Crop Residue Burning. *J. Environ. Sci. (China)* 20: 50–55.
- Chang, C.H., Liu, C.C., Wen, C.G., Cheng, I.F., Tam, C.K. and Huang, C.S. (2009). Monitoring Reservoir Water Quality with Formosat-2 High Spatiotemporal Imagery. *J. Environ. Monit.* 11: 1982–1992.
- Chen, K.S., Wang, H.K., Peng, Y.P., Wang, W.C. and Lai, C.H. (2008). Effects of Open Burning of Rice Straw on Concentrations of Atmospheric Polycyclic Aromatic Hydrocarbons in Central Taiwan. *J. Air Waste Manage. Assoc.* 58: 1318–1327.
- Chiu, J.C., Shen, Y.H., Li, H.W., Chang, S.S., Wang, L.C. and Chang-Chien, G.P. (2011). Effect of Biomass Open Burning on Particulate Matter and Polycyclic Aromatic Hydrocarbon Concentration Levels and PAH Dry Deposition in Ambient Air. *J. Environ. Sci. Health., Part A* 46: 188–197.
- Christian, T.J., Kleiss, B., Yokelson, R.J., Holzinger, R., Crutzen, P.J., Hao, W.M., Saharjo, B.H. and Ward, D.E. (2003). Comprehensive Laboratory Measurements of Biomass-Burning Emissions: 1. Emissions from Indonesian, African, and Other Fuels. *J. Geophys. Res.* 108: 4719–4732.
- Comber, A.J., Fisher, P.F. and Wadsworth, R.A. (2005). What is Land Cover? *Environ. Plann. B* 32:199–209.
- Elauria, J.C., Quejas, R.E.T., Cabrera, M.I., Liganor, R.V., Bhattacharya, S.C. and Predicala, N.L.J. (1999). Biomass as Energy Source in Philippines. *RERIC Int. Energy. J.* 21: 37–53.
- Elmore, A.J., Shi, X., Gorence, N.J., Li, X., Jin, H., Wang, F. and Zhang, X. (2008). Spatial Distribution of Agricultural Residue from Rice for Potential Biofuel Production in China. *Biomass Bioenergy* 32: 22–27.
- Estrellan, C.R. and Iino, F. (2010). Toxic Emissions from Open Burning. *Chemosphere* 80: 193–207.
- Gadde, B., Bonnet, S., Menke, C. and Garivait, S. (2009). Air Pollutant Emissions from Rice Straw Open Field Burning In India, Thailand and the Philippines. *Environ. Pollut.* 157: 1554–1558.
- Gregoire, J.M., Tansey, K. and Silva, J.M.N. (2003). The GBA2000 Initiative: Developing a Global Burnt Area Database from SPOT-VEGETATION Imagery. *Int. J. Remote Sens.* 24: 1369–1376.
- Gullett, B. and Touati, A. (2003). PCDD/F Emissions from Burning Wheat and Rice Field Residue. *Atmos. Environ.* 37: 4893–4899.
- Hao, W.M. and Liu, M.H. (1994). Spatial and Temporal Distribution of Tropical Biomass Burning. *Global Biogeochem. Cycles* 8: 495–503.
- Hays, M.D., Fine, P.M., Geron, C.D., Kleeman, M.J. and Gullett, B.K. (2005). Open Burning of Agricultural Biomass: Physical and Chemical Properties of Particle-Phase Emissions. *Atmos. Environ.* 39: 6747–6764.
- Hossain, A.M.M.M. and Park, K. (2012). Exploiting Potentials from Interdisciplinary Perspectives with Reference to Global Atmosphere and Biomass Burning Management. *Aerosol Air Qual. Res.* 12: 123–132.
- IPCC (2006). 2006 IPCC Guidelines for National Greenhouse Gas Inventories, Prepared by the National Greenhouse Gas Inventories Programme, Eggleston, H.S., Buendia, L., Miwa, K., Ngara, T. and Tanabe, K. (Eds.), Institute for Global Environmental Strategies, Japan.
- Ito, A. and Penner, J.E. (2004). Global Estimates of Biomass Burning Emissions Based on Satellite Imagery for the Year 2000. *J. Geophys. Res.* 109: D14S05, doi: 10.1029/2003JD004423.
- Jenkins, B.M. and Bhatnagar, A.P. (1991). On the Electric-Power Potential from Paddy Straw in the Punjab and the Optimal Size of the Power-Generation Station. *Bioresour. Technol.* 37: 35–41.
- Justice, C.O., Giglio, L., Korontzi, S., Owens, J., Morisette, J.T., Roy, D., Descloitres, J., Alleaume, S., Petitcolin, F. and Kaufman, Y. (2002). The MODIS Fire Products. *Remote Sens. Environ.* 83: 244–262.
- Kadam, K.L., Forrest, L.H. and Jacobson, W.A. (2000). Rice Straw as a Lignocellulosic Resource: Collection, Processing, Transportation, and Environmental Aspects. *Biomass Bioenergy* 18: 369–389.
- Kanabkaew, T. and Oanh, N.T.K. (2011). Development of Spatial and Temporal Emission Inventory for Crop Residue Field Burning. *Environ. Model. Assess.* 16: 453–464.
- Keshtkar, H. and Ashbaugh, L.L. (2007). Size Distribution of Polycyclic Aromatic Hydrocarbon Particulate Emission Factors from Agricultural Burning. *Atmos. Environ.* 41: 2729–2739.
- Lai, C.H., Chen, K.S. and Wang, H.K. (2009). Influence of Rice Straw Burning on the Levels of Polycyclic Aromatic Hydrocarbons in Agricultural County of Taiwan. *J. Environ. Sci. (China)* 21: 1200–1207.
- Lau, C.C. and Shiao, K.H. (1998). Combined Use of SPOT and GIS Data to Detect Rice Paddies, Asian Conference on Remote Sensing 1998, Manila, Philippine.
- Lillesand, T.M., Kiefer, R.W. and Chipman, J.W. (2004). *Remote Sensing and Image Interpretation*, 5th edition, John Wiley & Sons, NJ.
- Lin, L.F., Lee, W.J., Li, H.W., Wang, M.S. and Chang-Chien, G.P. (2007). Characterization and Inventory of PCDD/F Emissions from Coal-Fired Power Plants and Other Sources in Taiwan. *Chemosphere* 68: 1642–1649.
- Liu, C.C. (2006). Processing of FORMOSAT-2 Daily Revisit Imagery for Site Surveillance. *IEEE Trans. Geosci. Remote Sens.* 44: 3206–3214.
- Liu, C.C., Liu, J.G., Lin, C.W., Wu, A.M., Liu, S.H. and Shieh, C.L. (2007). Image Processing of FORMOSAT-2 Data for Monitoring the South Asia Tsunami. *Int. J. Remote Sens.* 28: 3093–3111.
- Liu, C.C. and Chen, P.L. (2009). Automatic Extraction of Ground Control Regions and Orthorectification of Remote Sensing Imagery. *Opt. Express* 17: 7970–7984.
- Liu, C.C., Wu, A.M., Yen, S.Y. and Huang, C.H. (2009a). Rapid Locating of Fire Points from Formosat-2 High Spatial Resolution Imagery: Example of the 2007 California Wildfire. *Int. J. Wildland Fire* 18: 415–422.

- Liu, C.C., Shieh, C.L., Wu, C.A. and Shieh, M.L. (2009b). Change Detection of Gravel Mining on Riverbeds from the Multi-Temporal and High-Spatial-Resolution Formosat-2 Imagery. *River Res. Appl.* 25: 1136–1152.
- Liu, C.C., Chang, Y.C., Huang, S., Yan, S.Y., Wu, F., Wu, A.M., Kato, S. and Yamaguchi, Y. (2009c). Monitoring the Dynamics of Ice Shelf Margins in Polar Regions with High-Spatial- and High-Temporal-Resolution Space-Borne Optical Imagery. *Cold Reg. Sci. Technol.* 55: 14–22.
- Liu, L.H., Jiang, J.Y. and Zong, L.G. (2011). Emission Inventory of Greenhouse Gases from Agricultural Residues Combustion: A Case Study of Jiangsu Province. *Environ. Sci.* 32: 1242–1248.
- NLSC (2011). Introduction to NLSC Affairs: National Land Surveying and Mapping Program, http://www.nlsc.gov.tw/websites/nlsceng/make_page.aspx?la=2&le=2&li=53&sno=166&le2=3&li2=166.
- NSPO (2012). Formosat-2 Image Distribution and Purchasing, <http://www.nspo.narl.org.tw/>. (in Chinese)
- Oanh, N.T.K., Ly, B.T., Tipayarom, D., Manandhar, B.R., Prapat, P., Simpson, C.D. and Liu, L.J.S. (2011). Characterization of Particulate Matter Emission from Open Burning of Rice Straw. *Atmos. Environ.* 45: 493–502.
- Shih, S.I., Lee, W.J., Lin, L.F., Huang, J.Y., Su, J.W. and Chang-Chien, G.P. (2008). Significance of Biomass Open Burning on the Levels of Polychlorinated Dibenzo-*p*-dioxins and Dibenzofurans in the Ambient Air. *J. Hazard. Mater.* 153: 276–284.
- Streets, D.G., Yarber, K.F., Woo, J.H. and Carmichael, G.R. (2003). Biomass Burning in Asia: Annual and Seasonal Estimates and Atmospheric Emissions. *Global Biogeochem. Cycles* 17: 1099–1119.
- Tipayarom, D. and Oanh, N.T.K. (2007). Effects from Open Rice Straw Burning Emission on Air Quality in the Bangkok Metropolitan Region. *Sci. Asia* 33: 339–345.
- TWEPA (2007). Project for Analyzing SIP Achievement of Local EPBs and Assistance on Performance Audit Works, Final Report. Environmental Protection Administration, Taiwan, ROC. (in Chinese)
- USEPA (1992). Emission Factor: Documentation for AP-42, Open Burning, Office of Air Quality Planning and Standards and Office of Air and Radiation (Ed.), U.S. Environmental Protection Agency, North Carolina.
- Venkataraman, C., Habib, G., Kadamba, D., Shrivastava, M., Leon, J.F., Crouzille, B., Boucher, O. and Streets, D.G. (2006). Emissions from Open Biomass Burning in India: Integrating the Inventory Approach with High-Resolution Moderate Resolution Imaging Spectroradiometer (MODIS) Active-Fire and Land Cover Data. *Global Biogeochem. Cycles* 20: GB2013.
- Viana, M., Lopez, J.M., Querol, X., Alastuey, A., Garcia-Gacio, D., Blanco-Heras, G., Lopez-Mahia, P., Pineiro-Iglesias, M., Sanz, M., Sanz, F., Chi, X. and Maenhaut, W. (2008). Tracers and Impact of Open Burning of Rice Straw Residues on PM in Eastern Spain. *Atmos. Environ.* 42: 1941–1957.
- Wu, Y.L., Li, H.W., Chien, C.H., Lai, Y.C. and Wang, L.C. (2010). Monitoring and Identification of Polychlorinated Dibenzo-*p*-dioxins and Dibenzofurans in the Ambient Central Taiwan. *Aerosol Air Qual. Res.* 10: 463–471.
- Yu, T.Y. (2012). Characterization of Ambient Air Quality During a Rice Straw Burning Episode. *J. Environ. Monit.* 14: 817–829.
- Zhang, H.F., Hu, D.W., Chen, J.M., Ye, X.N., Wang, S.X., Hao, J.M., Wang, L., Zhang, R.Y. and An, Z.S. (2011). Particle Size Distribution and Polycyclic Aromatic Hydrocarbons Emissions from Agricultural Crop Residue Burning. *Environ. Sci. Technol.* 45: 5477–5482.

Received for review, June 18, 2012

Accepted, October 23, 2012